Chinese Journal of Polymer Science Vol. 31, No. 10, (2013), 1359–1371

Chinese Journal of Polymer Science

SYNTHESIS OF AROMATIC DIAMINE-BASED BENZOXAZINES AND EFFECT OF THEIR BACKBONE STRUCTURE ON THERMAL AND FLAMMABILITY PROPERTIES OF POLYMERS*

Tao Zhang[a, c], Hong-qiang Yan[b**], Zheng-ping Fang[a, b] and Mao Peng[a]

[a] *MOE Key Laboratory of Macromolecular Synthesis and Functionalization, Department of Polymer Science and Engineering, Zhejiang University, Hangzhou 310027, China*

[b] *Lab of Polymer Materials and Engineering, Ningbo Institute of Technology, Zhejiang University, Ningbo 315100, China*

[c] *Department of Packaging Engineering, College of Materials and Textiles, Zhejiang Sci-tech University, Hangzhou 310018, China*

Abstract Three kinds of novel aromatic diamine-based benzoxazines containing naphthalene, propane-2,2-diyldibenzene and neopentyl groups in the backbone, respectively (designated as BAPNCP, BAPBACP and BAPNPGCP, respectively), were synthesized and characterized. In addition, the effects of backbone structures on curing behaviors of the monomers and thermal and flammability properties of the resulting polymers were systematically studied. The results indicated that BAPNPGCP displayed the highest enthalpy of the curing reaction associated with the ring-opening of benzoxazine, which was due to the effect of benzoxazine ring content per unit mass. Interestingly, the 5 wt% weight loss temperature and char residue after thermogravimetric test for poly(BAPNPGCP) were 8 °C and 7% higher than those of poly(BAPBACP). Meanwhile, the total heat release of poly(BAPNPGCP) was less than half of that for poly(BAPBACP), indicating the substantial effect of benzoxazine ring content on flammability and char formation. Furthermore, it was found that poly(BAPNCP) gave the best thermal stability and flame retardancy, which was due to the synergistic effect between naphthalene group and benzoxazine ring content. This study provides new insight into the curing behavior of benzoxazine and further understanding on the high performance of polybenzoxazine.

Keywords: Aromatic diamine-based benzoxazine; Thermal properties; Flammability properties.

INTRODUCTION

As a new class of promising thermosetting resins, polybenzoxazines have attracted substantial attention in the past decade due to their unique physical and chemical properties. They are more generally used as high performance materials in many fields, such as automotive, aerospace and construction industries[1], which require remarkable thermal stability and flame retardancy. Therefore, how to enhance thermal stability and flame retardancy of polybenzoxazines has become one of the main focuses of many endeavors. In general, introduction of additional functional groups into monomers and preparation of copolymers, polymer alloys and nanocomposites are widely used to obtain high performance polybenzoxazines[2, 3]. For example, benzoxazines have been prepared by introducing allyl[4], acetylene[3], nitrile[5], maleminde[6] and aldehyde groups[7] to the main chain or terminal position, which are usually derived from phenols or biphenols, monoamines and formaldehyde.

* This work was financially supported by the National Natural Science Foundation of China (No. 51103129), the National Basic Research Program of China ("973 Program", No. 2010CB631105), the Ningbo Natural Science Foundation (No. 2012A610084) and the Open Fund of Zhejiang Provincial Top Key Discipline of New Materials and Process Engineering (No. 20110939).

** Corresponding author: Hong-qiang Yan (闫红强), E-mail: yanhongqiang@nit.net.cn

Received October 15, 2012; Revised December 14, 2012; Accepted December 28, 2012
doi: 10.1007/s10118-013-1313-9

Copolymerization of benzoxazine with another reactive comonomer has been developed, such as urethane-benzoxazine[8] and benzoxazine-epoxy[9] copolymers, but the resulting systems often exhibit higher curing temperatures and viscosities than the neat polybenzoxazines[4, 10]. Various nanoparticles have been employed to prepare hybrid nanocomposites, such as clay[11], titania[12], silica[13], carbon nanotube[14] and polyhedral oligomeric silsesquioxane[15], but limitations exit in the dispersions of nanoparticles and performance improvements of nanocomposites.

Another simple and attractive approach is to synthesize aromatic diamine-based benzoxazines, which are derived from aromatic diamines, monophenols and formaldehyde. Recently, a series of novel monomers has been successfully synthesized by using high boiling point nonpolar solvent or a three-step synthetic method, which exhibits increased thermal stability of polymers relative to conventional polybenzoxazines due to the bond of nitrogen linkage to the other repeating unit[16, 17]. However, up to date, very limited success in preparing this kind of benzoxazine has been achieved mainly because of the difficulty of this benzoxazine ring-forming reaction, and the structure-property relationship has not yet been fully elucidated. In particular, effects of molecular stiffness and benzoxazine ring content on curing behaviors of the monomer and properties of the resulting polymer have not been profoundly concerned. In the present work, three kinds of typical aromatic diamine-based benzoxazines were designed and synthesized by the reaction of 4-hydroxybenzonitrile, paraformaldehyde, and pre-synthesized diamine compounds as shown in Scheme 1. The original idea was to alter the stiffness of molecular chain and benzoxazine ring content per unit mass by introducing naphthalene, propane-2,2-diyldibenzene or neopentyl group to the monomer backbone, so as to determine the effects of backbone structure on curing behaviors of the monomers and thermal and flammability properties of the resulting polymers.

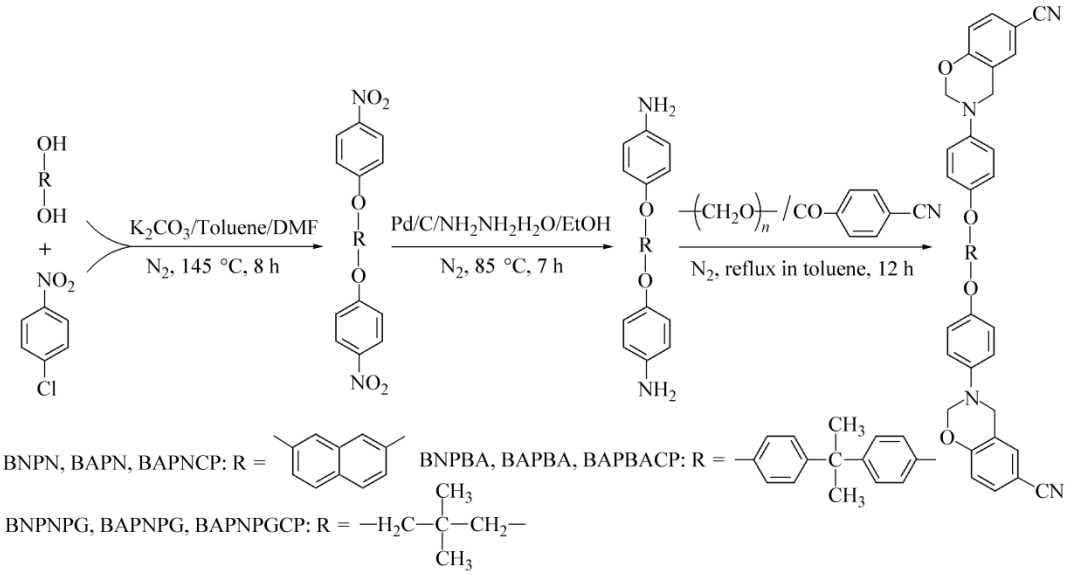

Scheme 1 Synthetic routes for aromatic diamine-based benzoxazine monomers containing naphthalene, propane-2,2-diyldibenzene and neopentyl group, respectively

EXPERIMENTAL

Materials

Neopentyl glycol (99%), 1-chloro-4-nitrobenzene (99.5%), 10% Pd/C and bisphenol A (> 99.0%) were purchased from Aladdin Chemistry Co., Ltd. Potassium carbonate (≥ 99.0%), *N*,*N*-dimethylformamide (DMF), ethanol, hydrazine hydrate (85%), paraformaldehyde (≥ 94.0%) and methanol were used as received from Sinopharm Chemical Reagent Co., Ltd. Toluene and 4-hydroxybenzonitrile (96%) were obtained from Hangzhou and Guangtuo Chemical Reagent Co., Ltd, respectively. 2,7-Dihydroxynaphthalene (97%) was

acquired from Acros Organics. The starting reagents were obtained from commercial suppliers and used directly without further purification.

Synthesis of Aromatic Dinitros

Following a slightly modified procedure[18, 19], 2,7-dihydroxynaphthalene (or bisphenol A, or neopentyl glycol, 0.1 mol) was added to a mixture of 1-chloro-4-nitrobenzene (0.22 mol) and potassium carbonate (0.12 mol) in 120 mL DMF and 30 mL toluene. The reaction mixture was heated at 145 °C for 8 h with stirring under nitrogen atmosphere, and the by-product water was collected in a Dean-Stark trap. The solution was filtered hot to remove inorganic salts, which were then washed several times with fresh DMF. Thereafter, the filtrate was concentrated under vacuum to give a thick solution, and poured into deionized water, yielding a precipitate, which was collected by filtration, dried under vacuum, and purified by recrystallization from ethanol/DMF mixture.

2,7-bis(4-nitrophenoxy)naphthalene (BNPN)

Green crystals; yield: 98%; mp (DSC): 167.6 °C (lit.[18] mp 167–168 °C); FTIR (KBr, 4000–400 cm^{-1}): 1512 cm^{-1}, 1338 cm^{-1} (N=O), 1238 cm^{-1} (C−O−C); ^{1}H-NMR (500 MHz, $CDCl_3$), δ: 7.08–8.25 (m, 14H, aromatic); Anal. calcd for $C_{22}H_{14}N_2O_6$: C 65.67, H 3.51, N 6.96; found: C 65.58, H 3.53, N 6.96.

4,4'-(propane-2,2-diyl)bis((4-nitrophenoxy)benzene) (BNPBA)

Yellow crystals; yield: 97%; mp (DSC): 119.1 °C (lit.[20] mp 120–124 °C); FTIR (KBr, 4000–400 cm^{-1}): 1515 cm^{-1}, 1342 cm^{-1} (N=O), 1245 cm^{-1} (C−O−C); ^{1}H-NMR (500 MHz, $CDCl_3$), δ: 1.74 (s, 6H, CH_3), 7.01–8.21 (m, 16H, aromatic); Anal. calcd for $C_{27}H_{22}N_2O_6$: C 68.93, H 4.71, N 5.95; found: C 68.69, H 4.74, N 5.99.

4,4'-((2,2-dimethylpropane-1,3-diyl)bis(oxy))bis(nitrobenzene) (BNPNPG)

White crystals; yield: 55%; mp (DSC): 163.6 °C; FTIR (KBr, 4000–400 cm^{-1}): 1504, 1336 cm^{-1} (N=O), 1263 cm^{-1} (C−O−C); ^{1}H-NMR (500 MHz, $CDCl_3$), δ: 1.20 (s, 6H, CH_3), 3.95 (s, 4H, CH_2), 6.96–8.20 (m, 8H, aromatic); Anal. calcd for $C_{17}H_{18}N_2O_6$: C 58.96, H 5.24, N 8.09; found: C 58.95, H 5.25, N 8.02.

Synthesis of Aromatic Diamines

Following a slightly modified procedure[18, 19], 10% Pd/C (0.25 g) was added to a mixture of BNPN (or BNPBA, or BNPNPG, 75 mmol) in 250 mL of ethanol. After the reaction mixture was stirred at 85 °C for 10 min under nitrogen atmosphere, hydrazine hydrate (85%, 80 mL) in ethanol (70 mL) was added dropwise over a period of 5 h, and the mixture was stirred for another 2 h. The solution was filtered to remove the 10% Pd/C and poured into deionized water, yielding a precipitate, which was collected by filtration, dried under vacuum, and then purified by recrystallization from ethanol.

4,4'-(naphthalene-2,7-diylbis(oxy))dianiline (BAPN)

Brown crystals; yield: 94%; mp (DSC): 167.9 °C (lit.[18] mp 166–67 °C); FTIR (KBr, 4000–400 cm^{-1}): 3394 cm^{-1}, 1630 cm^{-1} (N−H), 1215 cm^{-1} (C−O−C); ^{1}H-NMR (500 MHz, $CDCl_3$), δ: 4.99 (s, 4H, NH_2), 6.60–7.82 (m, 14H, aromatic); Anal. calcd for $C_{22}H_{18}N_2O_2$: C 77.17, H 5.30, N 8.18; found: C 76.85, H 5.31, N 8.17.

4,4'-((propane-2,2-diylbis(4,1-phenylene))bis(oxy))dianiline (BAPBA)

Yellow crystals; yield: 95%; mp (DSC): 127.1 °C (lit.[20] mp 128–130 °C); FTIR (KBr, 4000–400 cm^{-1}): 3403, 3338, 1610 cm^{-1} (N−H), 1226 cm^{-1} (C−O−C); ^{1}H-NMR (500 MHz, $CDCl_3$), δ: 1.63 (s, 6H, CH_3), 3.55 (br s, 4H, NH_2), 6.65–7.25 (m, 16H, aromatic); Anal. calcd for $C_{27}H_{26}N_2O_2$: C 79.00, H 6.38, N 6.82; found: C 78.98, H 6.48, N 6.89.

4,4'-((2,2-dimethylpropane-1,3-diyl)bis(oxy))dianiline (BAPNPG)

White crystals; yield: 92%; mp (DSC): 115.6 °C; FTIR (KBr, 4000–400 cm^{-1}): 3417, 3344, 1614 cm^{-1} (N−H), 1228 cm^{-1} (C−O−C); ^{1}H-NMR (500 MHz, $CDCl_3$), δ: 1.10 (s, 6H, CH_3), 3.12 (br s, 4H, NH_2), 3.74 (s, 4H, CH_2), 6.60–6.74 (m, 8H, aromatic); Anal. calcd for $C_{17}H_{22}N_2O_2$: C 71.30, H 7.74, N 9.78; found: C 71.26, H 7.86, N 9.71.

Synthesis of Aromatic Diamine-based Benzoxazines

Paraformaldehyde (60 mmol) and 4-hydroxybenzonitrile (22 mmol) were added to the mixture of BAPN (or BAPBA, or BAPNPG, 10 mmol) in 100 mL of toluene. After the reaction mixture was stirred at 110 °C for 12 h under nitrogen atmosphere, the solution was washed 3 times with 1N NaOH and 2 times with deionized water. Thereafter, the organic layer was separated, concentrated under vacuum to give a viscous solution, and then poured into ethanol, yielding a precipitate, which was collected by filtration, dried under vacuum, and extracted in a Soxhlet apparatus with methanol for 24 h.

3,3'-((naphthalene-2,7-diylbis(oxy))bis(4,1-phenylene))bis(3,4-dihydro-2H-benzo[e][1,3]oxazine-6-carbonitrile) (BAPNCP)

White powder; yield: 67%; FTIR (KBr, 4000–400 cm^{-1}): 1502 cm^{-1} (trisubstituted benzene ring stretching), 1246 cm^{-1} (asymmetric stretching vibration of C—O—C), 1030 cm^{-1} (symmetric stretching vibration of C—O—C), 937 cm^{-1} (out-of-plane C—H); ^{1}H-NMR (500 MHz, $CDCl_3$), δ: 4.60 (s, 4H, CH_2, oxazine), 5.39 (s, 4H, CH_2, oxazine), 6.86–7.75 (m, 20H, aromatic); Anal. calcd for $C_{40}H_{28}N_4O_4$: C 76.42, H 4.49, N 8.91; found: C 75.33, H 4.71, N 8.35.

3,3'-(((propane-2,2-diylbis(4,1-phenylene))bis(oxy))bis(4,1-phenylene))bis(3,4-dihydro-2H-benzo[e][1,3]oxazine-6-carbonitrile) (BAPBACP)

White powder; yield: 87%; mp (DSC): 133.0 °C; FTIR (KBr, 4000–400 cm^{-1}): 1500 cm^{-1} (trisubstituted benzene ring stretching), 1238 cm^{-1} (asymmetric stretching vibration of C—O—C), 1030 cm^{-1} (symmetric stretching vibration of C—O—C), 935 cm^{-1} (out-of-plane C—H); ^{1}H-NMR (500 MHz, $CDCl_3$), δ: 1.63 (s, 6H, CH_3), 4.58 (s, 4H, CH_2, oxazine), 5.38 (s, 4H, CH_2, oxazine), 6.82–7.42 (m, 22H, aromatic); Anal. calcd for $C_{45}H_{36}N_4O_4$: C 77.57, H 5.21, N 8.04; found: C 77.35, H 5.35, N 7.56.

3,3'-(((2,2-dimethylpropane-1,3-diyl)bis(oxy))bis(4,1-phenylene))bis(3,4-dihydro-2H-benzo[e][1,3]oxazine-6-carbonitrile) (BAPNPGCP)

White powder; yield: 80%; mp (DSC): 69.1 °C; FTIR (KBr, 4000–400 cm^{-1}): 1514 cm^{-1} (trisubstituted benzene ring stretching), 1238 cm^{-1} (asymmetric stretching vibration of C—O—C), 1032 cm^{-1} (symmetric stretching vibration of C—O—C), 933 cm^{-1} (out-of-plane C—H); ^{1}H-NMR (500 MHz, $CDCl_3$), δ: 1.08 (s, 6H, CH_3), 3.72 (s, 4H, CH_2), 4.53 (s, 4H, CH_2, oxazine), 5.33 (s, 4H, CH_2, oxazine), 6.77–7.40 (m, 14H, aromatic); Anal. calcd for $C_{35}H_{32}N_4O_4$: C 73.41, H 5.63, N 9.78; found: C 73.18, H 5.79, N 9.53.

Measurements

FTIR spectra (4000–400 cm^{-1}) were obtained from KBr pellets using a Bruker Vector-22 FTIR spectrometer with a resolution of 4 cm^{-1}. ^{1}H-NMR and ^{13}C-NMR spectra were recorded on a Bruker Avance DMX-500 MHZ spectrometer in $CDCl_3$ or DMSO-d_6, using TMS as the internal standard. Elemental analysis of carbon, hydrogen and nitrogen was obtained using a Flash EA 1112 ThermoFinnigan elemental analyzer. Differential scanning calorimetry (DSC) was carried out by using a NETZSCH DSC 200 PC unit with a scanning rate of 10 K/ min and a nitrogen flow rate of 60 mL/min from room temperature to 450 °C. The samples weighting about 3 mg were sealed between aluminum hermetic pans and lids for all tests. Thermogravimetric analysis (TGA) was performed with a NETZSCH TG 209 F1 thermogravimetric analyzer. 4–6 mg samples were tested in nitrogen atmosphere with a flow rate of 40 mL/min, from room temperature to 900 °C at a heating rate of 10 K/min. Microscale combustibility experiments were conducted with a Govmark MCC-2 microscale combustion calorimeter (MCC). The specimens (3–5 mg, in triplicate) were tested from 100 to 900 °C at a heating rate of 1 K/sec and oxygen/nitrogen flow rate was set at 20/80 mL/mL. Raman spectra were obtained using a Jobin-Yvon Labor Raman HR-800 Raman system by exciting a 514.5 nm Ar ion laser.

RESULTS AND DISCUSSION

Synthesis and Characterization of Benzoxazines

Three typical aromatic diamine-based benzoxazines were designed and synthesized for comprehensive studies,

which contain naphthalene, propane-2,2-diyldibenzene and neopentyl groups in the backbone, respectively. To synthesize the monomers, the diamines with different chemical structures are needed, which were synthesized according to Scheme 1. First, 1-chloro-4-nitrobenzene and potassium carbonate were coupled with 2,7-dihydroxynaphthalene, bisphenol A, or neopentyl glycol in order to obtain the dinitros with naphthalene, propane-2,2-diyldibenzene, or neopentyl group. Then, the dinitros were reduced efficiently using Pd/C catalyst to get the corresponding diamines. The structures of the obtained compounds were determined by FTIR, ^{1}H-NMR and elemental analysis, which are consistent with the proposed structures.

As illustrated in Scheme 1, the novel benzoxazines were synthesized by the reaction of 4-hydroxybenzonitrile, paraformaldehyde and the pre-synthesized aromatic diamines. All the obtained benzoxazines were with yields of 66%–87% and easily soluble in common solvents such as acetone, ethyl acetate and chloroform, but virtually insoluble in methanol, *n*-hexane and water. Structures of all the benzoxazines were confirmed by elemental analysis and spectral analysis.

As presented in Fig. 1, the FTIR spectra of all monomers showed characteristic absorptions of the benzoxazine structure at approximately 1500 (trisubstituted benzene ring stretching), 1238 (asymmetric stretching vibration of C—O—C), 1032 (symmetric stretching vibration of C—O—C) and 933 cm^{-1} (out-of-plane C—H), respectively. In the ^{1}H-NMR spectra shown in Fig. 2, the characteristic protons of the benzoxazine ring appeared at approximately 4.60 (Ar—CH_2—N) and δ = 5.30 (O—CH_2—N), respectively. Besides the chemical shifts that belong to the CH_2 and CH_3 group protons can also be clearly observed, confirming the formation of benzoxazines with different chemical structures. Furthermore, estimating the integration of the ^{1}H-NMR signals[10] at δ = 4.60 and δ = 5.39, the ratio of ring-closed to ring-opened for BAPNCP was about 99%. Following the same method, the ratios for BAPBACP and BAPNPGCP were 97% and 99%, respectively.

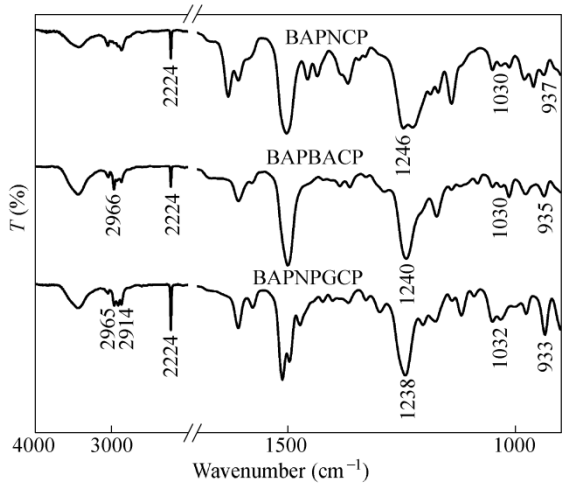

Fig. 1 FTIR spectra of BAPNCP, BAPBACP and BAPNPGCP

The chemical structures of all the benzoxazine monomers were further confirmed by ^{13}C-NMR, as shown in Fig. 3. In the ^{13}C-NMR spectrum of BAPNCP, the characteristic carbon resonances of the benzoxazine ring appeared at δ = 50.69 (Ar—CH_2—N) and δ = 80.76 (O—CH_2—N), respectively. As for BAPBACP, the characteristic carbon resonances of the benzoxazine ring appeared at δ = 50.98 (Ar—CH_2—N) and δ = 81.20 (O—CH_2—N) and that of the CH_3 group appeared at δ = 31.22. In the case of BAPNPGCP, the characteristic carbon resonances of the benzoxazine ring appeared at δ = 51.20 (Ar—CH_2—N) and δ = 81.73 (O—CH_2—N) and those of the CH_3 group and CH_2 group appeared at δ = 22.25 and 73.74, respectively.

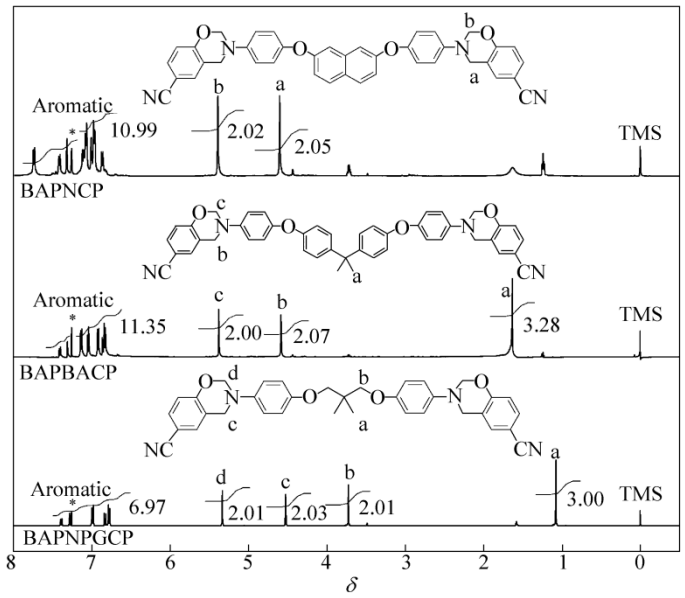

Fig. 2 ^{1}H-NMR spectra of BAPNCP, BAPBACP and BAPNPGCP in $CDCl_3$

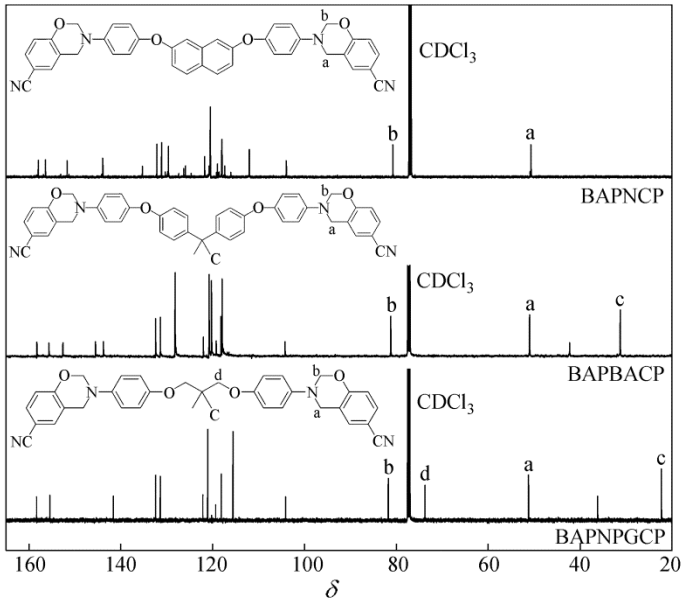

Fig. 3 ^{13}C-NMR spectra of BAPNCP, BAPBACP and BAPNPGCP in $CDCl_3$

Curing Behavior of Benzoxazines

DSC was carried out to study the effect of backbone structures on curing behavior of the benzoxazines as shown in Fig. 4(a) and Table 1. All monomers exhibited T_p at around 220 °C, which was attributed to the ring-opening polymerization of benzoxazine. DSC thermogram of BAPNPGCP showed a single sharp exothermic peak with T_i at 186 °C and T_p at 223 °C, and the ΔH value was 253 J/g. BAPBACP exhibited a broader peak starting at 172 °C with T_p at 221 °C, and the ΔH value was 159 J/g. For BAPNCP, two exotherms were observed. The T_i of the first exotherm was 155 °C with T_p at 218 °C, and the T_i of the second one was 265 °C with T_p at 302 °C. The ΔH values for the two exotherms were 120 and 84 J/g, respectively, so the total ΔH value for BAPNCP was 204 J/g. Furthermore, the second broad exothermic peak for BAPNCP may be the split one ascribed to the

uncured residual in the first region, which was due to the hindered chain mobility because of the higher molecular rigidity imparted by the naphthalene ring. These results reveal that introduction of rigid group to the monomer backbone hinders the chain mobility, resulting in longer polymer interchain distances and hence inhibits the curing reaction. A similar effect was observed for the difference between T_i and T_p of the exothermic peak. From BAPNPGCP to BAPNCP, the difference increased orderly, indicating an evident influence of the structural modification of the monomer backbone on the curing process. Another interesting observation was that the ΔH value decreased monotonically as the molecular weight of benzoxazine monomer increased, confirming the effect of the benzoxazine ring content per unit mass[21].

Table 1. DSC analysis of the benzoxazine monomers[a]

Sample	T_i (°C)	T_p (°C)	ΔH (J/g)
BAPNCP	155, 265	218, 302	120, 84
BAPBACP	172	221	159
BAPNPGCP	186	223	253

[a]T_i: onset temperature of the exothermic peak; T_p: maximum temperature of the exothermic peak; ΔH: enthalpy of the curing reaction

The curing behavior of the benzoxazines was also monitored by DSC after each cure stage as shown in Figs. 4(b–d). For comparison, the monomers were cured stepwise at 130, 160, and 190 °C for 2 h each, and then postcured at 220 and 250 °C for 1 h in an air oven. In the case of BAPBACP and BAPNPGCP, the exothermic peaks corresponding to the ring-opening polymerization of benzoxazine decreased gradually after each cure stage and disappeared completely after 190 °C for 2 h cure, suggesting the completion of curing. Compared to the other two samples, the first exothermic peak for BAPNCP changed similarly, but the second one remained almost unchanged until after 220 °C and disappeared completely after 250 °C for 1 h cure.

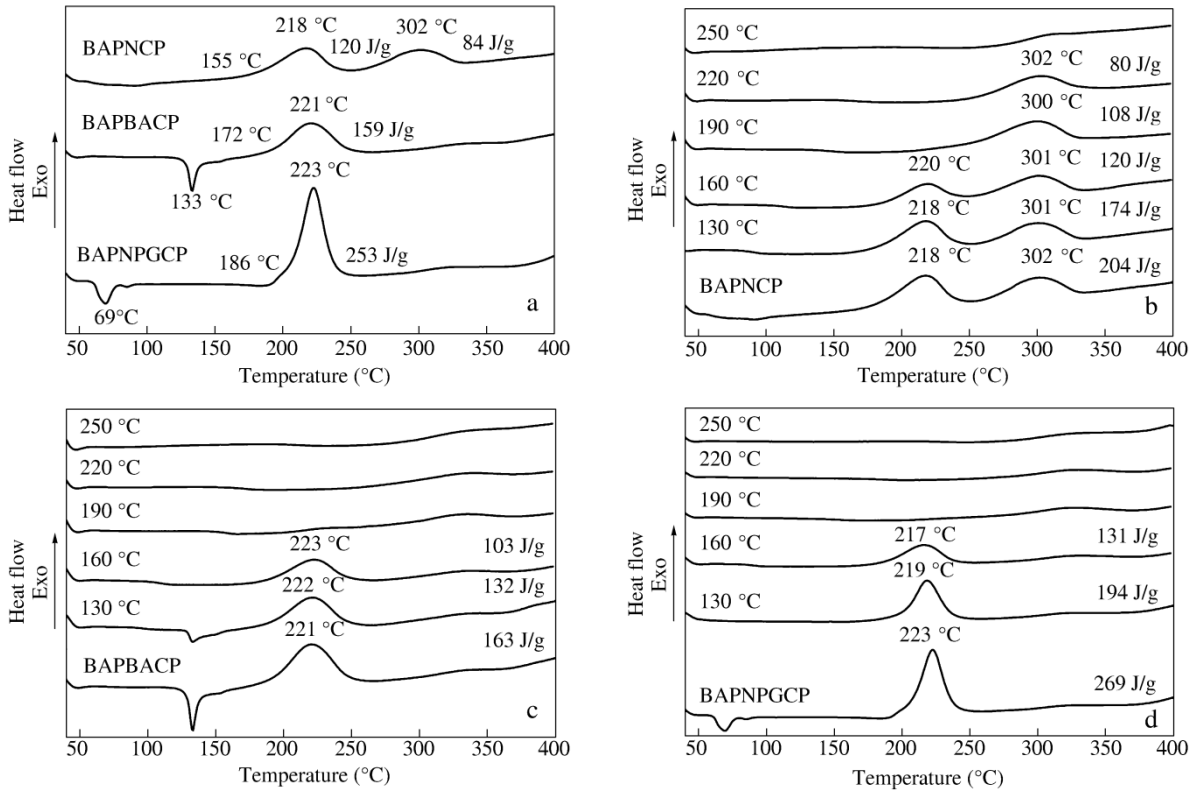

Fig. 4 DSC thermograms of (a) BAPNCP, BAPBACP and BAPNPGCP, (b) BAPNCP after each cure stage, (c) BAPBACP after each cure stage and (d) BAPNPGCP after each cure stage

In order to gain more insight into these processes, we also monitored the curing behavior by FTIR spectroscopy as shown in Fig. 5. For BAPNPGCP, the characteristic absorption bands ascribed to benzoxazine structure at 933, 1032, and 1238 cm^{-1} decreased gradually after each cure stage and disappeared after curing at 190 °C for 2 h. Meanwhile, the band at 1514 cm^{-1} attributed to the trisubstitued benzene ring decreased gradually, and correspondingly a new band appeared at 1506 cm^{-1} attributed to the tetrasubstituted benzene ring, confirming the ring-opening polymerization of benzoxazine and formation of the polybenzoxazine network[10, 22]. In the case of BAPNCP and BAPBACP, the characteristic absorption bands ascribed to benzoxazine structure disappeared gradually upon the ring-opening polymerization, showing similar curing behavior to that for BAPNPGCP. However, the absorption band at approximately 1238 cm^{-1} did not disappear completely, which was probably due to the asymmetric stretching vibration of aryl ether linkages which overlapped with that of C—O—C for benzoxazine structure[23]. Furthermore, BAPNCP showed little change in intensity of the absorption band at 1502 cm^{-1} after each cure stage, which was probably due to the trisubstituted benzene ring of the naphthalene ring which overlaps with that of tetrasubstituted benzene ring, demonstrating the difficulty for the formation of polybenzoxazine network. In addition, characteristic band at 2224 cm^{-1} (stretching vibration of C≡N) remained almost unchanged after each cure stage, even after curing at 250 °C for 1 h, which has been reported in the literature[5]. Figure 5(d) shows the proposed structure for the thermosets obtained by the thermally activated ring opening polymerization.

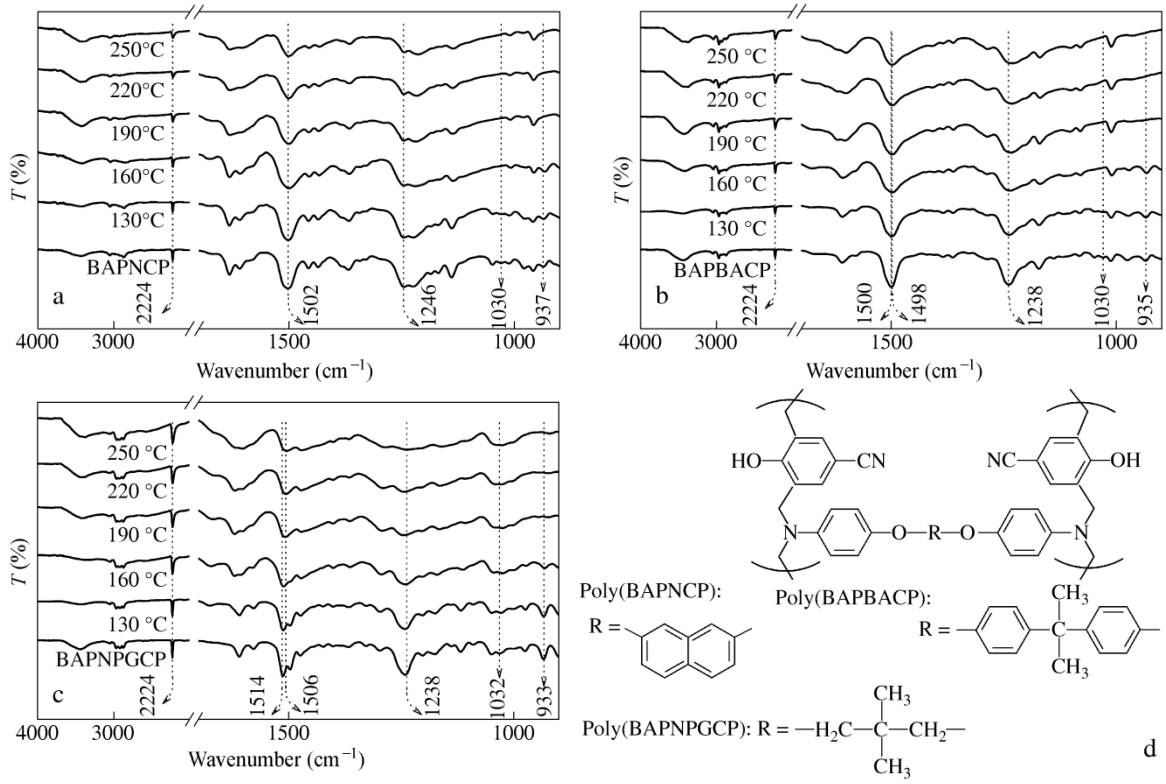

Fig. 5 FTIR spectra of BAPNCP (a), BAPBACP (b) and BAPNPGCP (c) after each cure stage in the 4000–900 cm^{-1} region; proposed structure of poly(BAPNCP), poly(BAPBACP) and poly(BAPNPGCP) (d)

Thermal Properties of Polybenzoxazines

An interesting observation was that poly(BAPNPGCP) possessed higher thermal stability compared to poly(BAPBACP) under nitrogen atmosphere. The decomposition temperatures $T_{5\%}$ and $T_{10\%}$ of poly(BAPNPGCP) were 376 and 416 °C, respectively, and the char residue at 900 °C was 53 %. Even with propane-2,2-diyldibenzene groups, the $T_{5\%}$ and $T_{10\%}$ for poly(BAPBACP) were still lower than those of

poly(BAPNPGCP) (Fig. 6a and Table 2). According to literature reports[6], the initial decomposition is ascribed to the breakage of Mannich bridges and the following release of aniline derivatives. Therefore, the higher thermal stability in the initial stage for poly(BAPNPGCP) is most likely due to the higher benzoxazine ring content per unit mass, which causes an increase in the anchoring points of aniline derivatives. In addition, the char residue at 900 °C for poly(BAPNPGCP) was also higher than that of poly(BAPBACP), which was consistent with the results made by Ishida *et al.*[24] on the diamine-based maleimide benzoxazines with different aromatic structure in the backbone, demonstrating the significant effect of benzoxazine ring content per unit mass on the char residue. However, for the purpose of comprehensive comparison, we synthesized BAPNCP with naphthalene group in the backbone. The $T_{5\%}$, $T_{10\%}$ and char residue at 900 °C of poly(BAPNCP) were significantly higher than those of poly(BAPNPGCP). This increased thermal stability may arise substantially from naphthalene ring, which has prominent chain stiffening and thermal stability. Therefore, it can be expected that if benzoxazines with higher benzoxazine ring content and much more thermally stable groups are prepared, the thermal stability of the corresponding polymers should be improved.

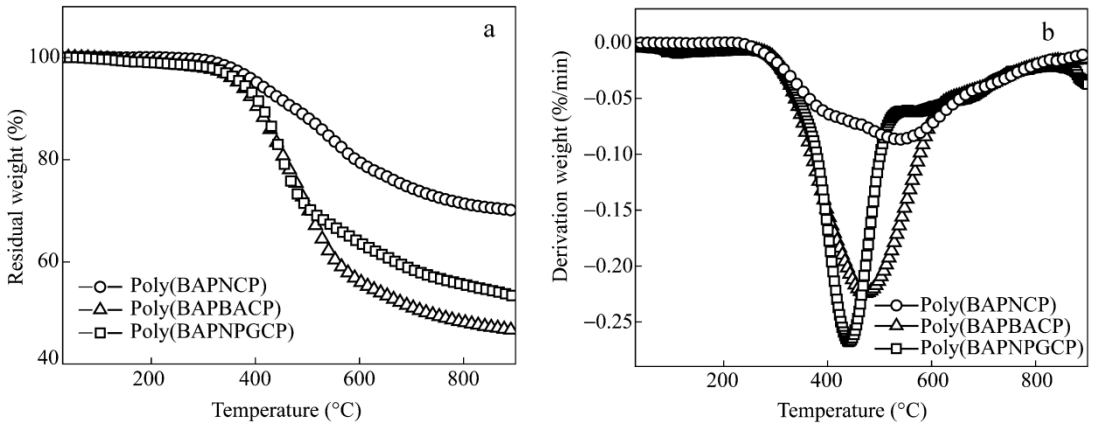

Fig. 6 TGA curves (a) and DTG curves (b) for poly(BAPNCP), poly(BAPBACP) and poly(BAPNPGCP) under nitrogen atmosphere

Table 2. Thermal properties of the polybenzoxazines[a]

Sample	$T_{5\%}$ (°C)	$T_{10\%}$ (°C)	$T_{20\%}$ (°C)	T_{max} (°C)	Char (%) at 900 °C
Poly(BAPNCP)	406	478	596	541	70
Poly(BAPBACP)	368	408	458	473	46
Poly(BAPNPGCP)	376	416	454	441	53

[a]$T_{5\%}$: temperature for which the weight loss is 5 wt%; $T_{10\%}$: temperature for which the weight loss is 10 wt%; $T_{20\%}$: temperature for which the weight loss is 20 wt%; T_{max}: temperature for which the weight loss is at its maximum; Char: char yield at 900 °C under nitrogen atmosphere.

As shown in the differential thermogravimetric (DTG) curves (Fig. 6b), poly(BAPNCP) showed a relatively intense degradation process centered around 540 °C, a noticeable secondary process at around 400 °C and a weak broad shoulder from 650 to 800 °C. Similarly, there was a relatively intense degradation process centered around 470 and 440 °C for poly(BAPBACP) and poly(BAPNPGCP), respectively. It is interesting to note that the decomposition temperature T_{max} for poly(BAPBACP) is higher than that of poly(BAPNPGCP), which is contrary to the result of TGA in the initial stage. This result was mostly due to the breakage of aryl ether linkages and the following release of organic fragments[21], which showed a sudden weight loss in the range of 430–500 °C for poly(BAPNPGCP). In the case of poly(BAPNCP), the decomposition temperature T_{max} was much higher than that of the other two polybenzoxazines, which was consistent with the result of TGA in the initial stage.

Flammability Properties of Polybenzoxazines

In order to further analyze the correlation between the backbone structure and flammability, we simulated the anaerobic pyrolysis and a subsequent reaction of the volatile pyrolysis products with nitrogen/oxygen (80/20) gas mixture under high temperatures by MCC. The heat release rate is plotted as a function of temperature in Fig. 7(a), and the results are summarized in Table 3. Observed from the flammability parameters measured, the remarkable differences are char residue and THR. The char residue after MCC test for poly(BAPNPGCP) was 10% higher than that of poly(BAPBACP), and the THR was less than half that for poly(BAPBACP), indicating that benzoxazine ring content has a substantial effect on flammability and char formation. Another contributing factor was the thermally stable group, as shown by poly(BAPNCP) containing naphthalene ring, which showed a char residue increase of 15% and 1 % decrease of the THR as compared with poly(BAPNPGCP).

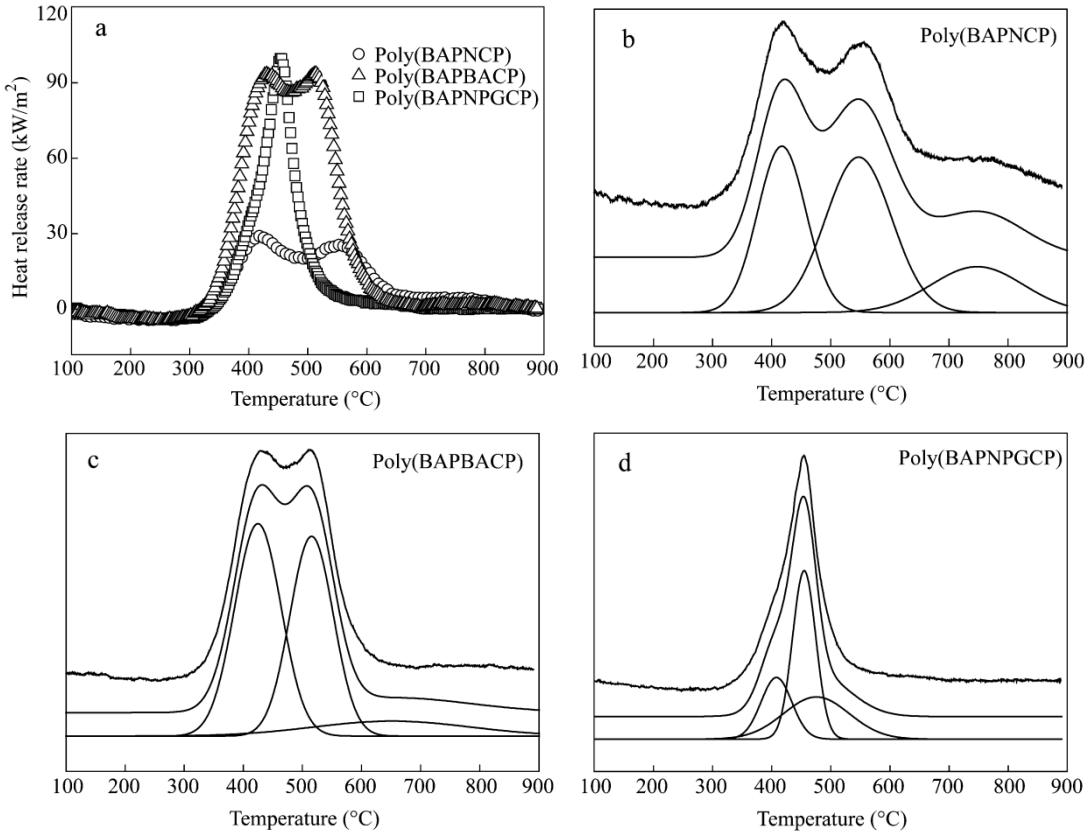

Fig. 7 Heat release rate curves for poly(BAPNCP), poly(BAPBACP) and poly(BAPNPGCP) (a), and curve fittings of poly(BAPNCP) (b), poly(BAPBACP) (c) and poly(BAPNPGCP) (d) including original curve, modeled peaks and fitted curves

With a view to compare the combustion process, the heat release rate curves were fitted by Guassian curves, as presented in Fig. 7(b–d), showing that the degradation of all the samples occurs through three steps. Compared to poly(BAPBACP), the PHRR of poly(BAPNPGCP) in the first stage decreased remarkably from 96.55 to 39.55 W/g, although it started at a relatively lower temperature, reflecting slow heat release rate by hindering release of aniline derivatives. In the second stage, the PHRR of poly(BAPNPGCP) occurred at a lower temperature than that of poly(BAPBACP), probably because of the breakage of aryl ether linkage and the rapid release of organic fragments, which was also found in TGA results. However, poly(BAPNCP) showed the highest T_{PHRR} value among all polymers, which was believed to be due to the synergistic effect between naphthalene group and benzoxazine ring content on the heat release and flammability. These observations are interesting and warrant the following discussion.

Table 3. Microscale combustion calorimetry results for the polybenzoxazines[a]

Sample	Char residue (%)	PHRR (s) (W/g)	T_{PHRR} (s) (°C)	THR (kJ/g)
Poly(BAPNCP)	72.80 ± 1.82	31.70 ± 1.07, 29.42 ± 1.86, 7.55 ± 0.50	423.31 ± 4.14, 547.52 ± 3.40, 748.90 ± 3.51	6.6 ± 0.4
Poly(BAPBACP)	48.04 ± 0.37	96.55 ± 1.63, 96.02 ± 4.91, 6.48 ± 0.93	431.79 ± 3.47, 507.01 ± 1.09, 651.59 ± 1.52	17.0 ± 1.2
Poly(BAPNPGCP)	57.84 ± 1.50	39.55 ± 4.52, 97.49 ± 5.13, 18.45 ± 1.45	407.85 ± 6.02, 453.78 ± 9.16, 475.78 ± 5.08	7.5 ± 0.5

[a] THR: total heat release; PHRR: peak heat release rate; T_{PHRR}: temperature at the peak heat release rate; Char residue: obtained from the difference between the mass before and after test.

Analysis of the Collected Char Residues

To better understand the evolution of chemical structure during thermal degradation, the TGA tests of all the samples were stopped at the decomposition temperatures $T_{5\%}$, $T_{10\%}$, $T_{20\%}$, T_{max} and 900 °C, respectively, and the collected solid residues were analyzed by FTIR spectroscopy. The thermal degradation processes of all the samples were shown to be essentially identical, so only poly(BAPNCP) is presented in Fig. 8 as a representative. As can be seen, the band intensity of 1217 cm^{-1} (stretching vibration of aryl ether linkages)[18] changed little below $T_{10\%}$, decreased slowly in response to the temperature increase and disappeared completely at 900 °C. However, the peak at 1138 cm^{-1} (stretching vibration of C—N—C)[25] weakened clearly in intensity as the temperature increased and almost vanished at T_{max}. This result indicates that the breakage of Mannich bridges is much faster than that of aryl ether linkages, which are consistent with the TGA and MCC results. Notably, the sharp peak at 2224 cm^{-1} (stretching vibration of C≡N) can still be obviously observed at $T_{20\%}$, signifying the higher thermal stability of the terminal phenylnitrile functional group.

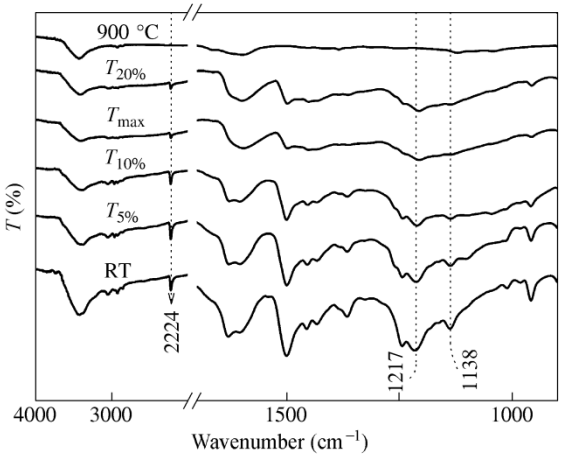

Fig. 8 FTIR spectra of poly(BAPNCP) at different decomposition temperatures in the 4000–900 cm^{-1} region

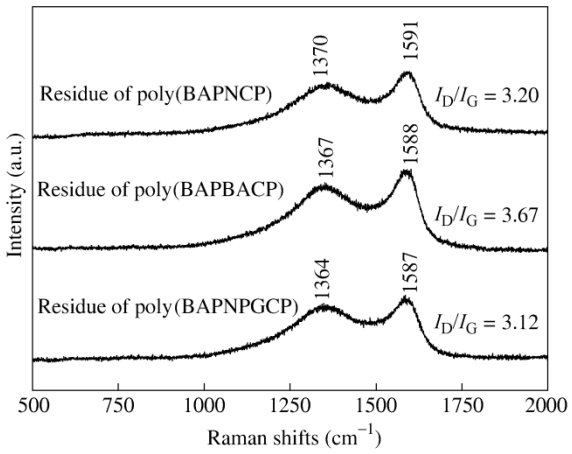

Fig. 9 Raman spectra for the char residues of polybenzoxazines
The wavenumbers of D and G bands are shown at their peaks respectively, and the intensity ratio of D band to G band is given on the right side of each spectrum.

TGA residues at 900 °C for all the polybenzoxazines were also collected and analyzed by Raman spectroscopy, as shown in Fig. 9 for comparison. The spectra clearly showed the existence of two peaks at around 1370 and 1580 cm^{-1}, which are believed to be assigned to D and G bands, respectively. It is well-known that the D and G bands are attributed to amorphous and crystalline graphitic carbon, respectively, and the intensity ratio of D band to G band (I_D/I_G) can reflect well the graphitization degree of carbon materials[26, 27]. For

poly(BAPNCP), poly(BAPBACP) and poly(BAPNPGCP), the I_D/I_G values of the residues were 3.20, 3.67 and 3.12 respectively. Poly(BAPNPGCP), with the highest content of benzoxazine ring, had the lowest I_D/I_G value for the residues. Thus, the residues of poly(BAPNPGCP) showed relatively higher graphitization degree than the other two samples.

CONCLUSIONS

A series of novel aromatic diamine-based benzoxazines, BAPNCP, BAPBACP and BAPNPGCP, has been successfully synthesized and characterized. The resulting polybenzoxazines showed good thermal stability and flame retardancy. In addition, turning backbone structure of aromatic diamine-based benzoxazines can have a remarkable effect on curing behaviors of the monomers and properties of the polymers. In this work, the highest ΔH value attributed to the ring-opening polymerization of benzoxazine was found in BAPNPGCP, whereas the lowest amount was found in BAPBACP. Accordingly, the decomposition temperature $T_{5\%}$ and char residue after thermogravimetric test for poly(BAPNPGCP) were 8 °C and 7% higher than those of poly(BAPBACP), and the THR of poly(BAPNPGCP) was less than half of that for poly(BAPBACP), suggesting the increase in anchoring points of decomposition derivatives for poly(BAPNPGCP). However, the thermal stability and level of flame retardancy for poly(BAPNCP) were the highest among the three samples, which was probably due to synergistic effect between naphthalene group and benzoxazine ring content. Thus, to improve thermal stability and flame retardancy of polybenzoxazines, a synergistic optimization of the thermally stable group and benzoxazine ring content is crucial. As the content of thermally stable group and benzoxazine ring changes, the properties of the resulting polymers should also be tailored.

REFERENCES

1 Ishida, H. and Rodriguez, Y., Polymer, 1995, 36(16): 3151
2 Chernykh, A., Agag, T. and Ishida, H., Macromolecules, 2009, 42(14): 5121
3 Andreu, R., Espinosa, M.A., Galià, M., Cádiz, V., Ronda, J.C. and Reina, J.A., J. Polym. Sci. Part A: Polym. Chem., 2006, 44(4): 1529
4 Santhosh Kumar, K.S., Reghunadhan Nair, C.P., Radhakrishnan, T.S. and Ninan, K.N., Eur. Polym. J., 2007, 43(6): 2504
5 Qi, H., Ren, H., Pan, G., Zhuang, Y., Huang, F. and Du, L., Polym. Adv. Technol., 2009, 20(3): 268
6 Agag, T. and Takeichi, T., J. Polym. Sci. Part A: Polym. Chem., 2006, 44(4): 1424
7 Gu, Y. and Ran, Q. C., J. Polym. Sci. Part A: Polym. Chem., 2011, 49(7): 1671
8 Rimdusit, S., Bangsen, W. and Kasemsiri, P., J. Appl. Polym. Sci., 2011, 121(6): 3669
9 Jubsilp, C., Punson, K., Takeichi, T. and Rimdusit, S., Polym. Degrad. Stab., 2010, 95(6): 918
10 Agag, T. and Takeichi, T., J. Polym. Sci. Part A: Polym. Chem., 2007, 45(10): 1878
11 Gârea, S.A., Iovu, H., Nicolescu, A. and Deleanu, C., Polym. Test., 2009, 28(3): 338
12 Agag, T., Tsuchiya, H. and Takeichi, T., Polymer, 2004, 45(23): 7903
13 Fan, X.Y., Yan, C., Li, J. and Shen, S.Z., J. Appl. Polym. Sci., 2011, 120(3): 1525
14 Chen, Q., Xu, R.W. and Yu, D.S., Polymer, 2006, 47(22): 7711
15 Chen, Q., Xu, R.W., Zhang, J. and Yu, D.S., Macromol. Rapid. Commun., 2005, 26(23): 1878
16 Agag, T., Jin, L. and Ishida, H., Polymer, 2009, 50(25): 5940
17 Lin, C.H., Chang, S.L., Hsieh, C.W. and Lee, H.H., Polymer, 2008, 49(5): 1220
18 Leu, T.S. and Wang, C.S., Polymer, 2002, 43(25): 7069
19 Faghihi, K., Nourbakhsh, M. and Hajibeygi, M., Chinese J. Polym. Sci., 2010, 28(6): 941
20 Qi, G., Zhang, X.H., Chen, S., Chen, T., Sun, X.K. and Liu, F., J. Appl. Polym. Sci., 2007, 106(3): 1632
21 Agag, T., Geiger, S., Alhassan, S.M., Qutubuddin, S. and Ishida, H., Macromolecules, 2010, 43(17): 7122
22 Agag, T. and Takeichi, T., Macromolecules, 2001, 34(21): 7257

23 Zhang, L., Peng, H., Sui, J., Soeller, C., Kilmartin, P.A. and Travas-Sejdic, J., J. Phys. Chem. C., 2009, 113(21): 9128
24 Jin, L., Agag, T. and Ishida, H., Eur. Polym. J., 2010, 46(2): 354
25 Brunovska, Z. and Ishida, H., J. Appl. Polym. Sci., 1999, 73(14): 2937
26 Xu, L., Fang, Z., Song, P.A. and Peng, M., Plasma Process. Polym., 2010, 7(9-10): 785
27 Hsieh, C.T., Teng, H., Chen, W.Y. and Cheng, Y.S., Carbon, 2010, 48(15): 4219